Renewable Energy 218 (2023) 119251

Contents lists available at ScienceDirect

Renewable Energy

journal homepage: www.elsevier.com/locate/renene

Environmental impact of cogeneration in binary geothermal plants

Kathrin Menberg [a,*], Florian Heberle [b], Hannah Uhrmann [b], Christoph Bott [c], Sebastian Grünäugl [a], Dieter Brüggemann [b], Peter Bayer [c]

[a] Institute of Applied Geosciences (AGW), Karlsruhe Institute of Technology (KIT), Kaiserstraße 12, 76131, Karlsruhe, Germany
[b] Center of Energy Technology (ZET), University of Bayreuth, Prof.-Rüdiger-Bormann-Strasse 1, 95440, Bayreuth, Germany
[c] Department of Applied Geology, Martin Luther University Halle-Wittenberg, Von-Seckendorff-Platz 3, 06120, Halle, Germany

ARTICLE INFO

Keywords:
Geothermal energy
Combined heat and power
Life cycle assessment
Binary power plant
District heating network

ABSTRACT

Cogeneration of power and heat from geothermal resources is considered an environmentally alternative to conventional energy, yet the environmental benefits of combined heat and power (CHP) binary plants have so far not been quantified. Here, we apply life cycle assessment to quantify the environmental impacts for three CHP concepts for the hydrothermal plant of Kirchstockach, Germany. A comprehensive, site-specific life cycle inventory is compiled, which encompasses components and processes needed for the plant-specific refrigerant, as well as for construction and operation of a district heating network (DHN). Results show that the CHP options perform equally well in terms of environmental emissions for heat generation (3.9–4.0 gCO_2-eq./kWh_{th}) and vastly outperform conventional, fossil heat sources. Although cogeneration reduces the amount of generated electricity, the corresponding increase in the environmental burden is found to be minimal (4.3–6.6 gCO_2-eq./kWh_{th}). Different schemes to share the environmental burden of auxiliary energy between heat and power output showed no significant difference, as long as the auxiliary energy is supplied by the binary plant itself. As 78% of the non-renewable energy demand of the generated heat in Kirchstoackach are associated with DHN construction, sites with an existing network will particularly benefit from cogeneration of geothermal heat and power.

1. Introduction

The utilization of geothermal resources is considered an environmentally friendly choice for generation of electricity and heat. In particular, closed-loop circulation of geothermal fluids in so-called binary systems prevents critical on-site emissions of carbon dioxide and methane, which represent incondensable gases that are often released to the atmosphere at high-enthalpy dry or flash-steam power plants [1–4]. In general, binary systems are suited for electricity generation at temperatures of 110–170 °C. This is a characteristic range for enhanced geothermal systems and groundwater in deep sedimentary basins, and utilization is most effective if power plants accomplish cogeneration of heat [5–9]. When cogeneration, or combined heat and power (CHP) systems are employed, economic benefits are maximized by both feeding power into an electricity grid and thermal energy into a heat supply network. In addition, this minimizes the environmental footprint of each unit of energy produced. Thus, proper configuration of the cogeneration technology is key for a techno-economic and environmental system optimization [6,10–14].

The standard conversion technology applied in binary power plants is the Organic Rankine Cycle (ORC). The geothermal fluid of the reservoir is circulated from production to injection wells, and heat transfer to the secondary cycle is realized via heat exchangers. Hereby, saturated or slightly superheated vapour of the ORC working fluid is provided and subsequently expanded in the turbine to generate electric power. In addition, heat can be extracted from the geothermal circuit to supply thermal users directly or via a district heating network (DHN). While the ORC system is designed as a closed cycle, similar to the geothermal loop, commonly small fractions of the refrigerant are continuously lost and need to be refilled. This may be caused by leaking seals or slip-ups during regular maintenance. Mean annual leakage rates are rarely reported and only expected to be within the range of a few percent [13,15–19]. However, due to a considerable global warming potential (GWP) of many of the refrigerants used in practice (e.g., R134a), these can contribute substantially to the overall environmental performance of a plant. Still, in most previous studies analysing the environmental aspects of geothermal plants, this has been neglected [5,8,14,20].

The customary formalism for environmental analysis is life cycle assessment (LCA) according to the ISO 14040–14049 series of standards

* Corresponding author.
E-mail address: menberg@kit.edu (K. Menberg).

https://doi.org/10.1016/j.renene.2023.119251
Received 15 October 2022; Received in revised form 23 August 2023; Accepted 29 August 2023
Available online 30 August 2023

Abbreviations

AP	Acidification Potential
CHP	Combined Heat and Power
CCHP	Combined Cooling Heat and Power
DHN	District Heating Network
EGS	Enhanced Geothermal System
EP	Eutrophication Potential
GHG	Greenhouse Gas
GWP	Global Warming Potential
HT	High Temperature
LCA	Life Cycle Assessment
LCI	Life Cycle Inventory
LCIA	Life Cycle Inventory Analysis
LT	Low Temperature
ORC	Organic Rankine Cycle

[21,22]. For a given unit performance, scope and system boundary, a life cycle inventory (LCI) is developed that quantifies all related environmental flows, primary energy consumption, resource use and emissions. Within the subsequent life cycle impact assessment (LCIA), multiple effects are expressed by standardized indicators with respect to common areas of environmental concern, and these are discussed together in the final interpretation phase.

During the last decade, the number of studies dealing with LCA of geothermal systems has significantly increased, covering low-enthalpy technologies [15,23,24], geothermal storage applications [25], as well as binary and flash-steam power plants [1,4,5,9,26–31]. Cogeneration was subject to a study by Karlsdottir et al. [12], which examined the environmental impacts with respect to 1 kWh_{el} and 1 kWh_{th} produced at the flash-steam plant Hellisheiði in Iceland. It was demonstrated that, after the construction phase, emissions of geothermal gases contribute substantially to the impact categories global warming potential, acidification and human toxicity for this location. The distinction of the environmental effects with respect to both equally vital outputs from the energy conversion, electricity and heat, was critically discussed, and accordingly the choice of the allocation method. In that work, joint input processes were allocated based on their share in the overall useful energy production, but also the economic values of both useful energy products or the exergy could be applied as reference [5,15,32].

Cogeneration by large-scale binary plants is common practice but rarely considered in previous LCA studies. This is especially the case, when comparisons amongst different LCA applications are made, and when the exergy associated with heat production is low or considered negligible [33]. Ruzzenenti et al. [34] compare LCAs for ORC-based electricity and thermal energy production for a micro-size system (50 kW) that combines geothermal with solar energy, but their study does not consider any particular allocation approach. Also, a small-scale geothermal system for a combined cooling, heat and power (CCHP) application was analyzed by Chaiyat et al. [35]. There, the conducted LCA is based on the existing geothermal plant San Kamphaeng (Thailand). The system produces 10 kW_{el} of power, 9.84 kW of cooling, and 18.77 kW of heating. The results show lower emission equivalents compared to combined cycle-gas turbine and coal power plants.

Germany was found to have a large potential for CHP from hydrothermal resources in terms of technical potential (12.2 PWh_{el}, 16.7 $PWht_{h}$), and considering sustainable reservoir management in terms of economic potential (9.1 PWh_{el}, 12.5 $PWht_{h}$) [36]. The environmental benefits of CHP systems in Germany have not been quantified yet. However, on-site conditions can be considered representative for other regions with deep sedimentary basins, where relatively low operational temperatures of commonly less than 150 °C can be realized. Below this temperature, low conversion efficiency and exergy favour cogeneration or even full use for seasonal heating applications.

In this work, the objective is to develop and demonstrate an LCA framework for addressing cogeneration of heat in binary geothermal power plants utilizing hydrothermal reservoirs. For this purpose, three different allocation schemes are compared and applied to a binary power plant operated in the Southern-German Molasse basin. We build upon a previous assessment framework presented for the Kirchstockach plant [37], and further refine the LCI by improved operational parameters, working fluid application and construction of a local DHN. Also, we assess the environmental effects of different schemes for auxiliary power supply of the ORC and CHP component within the LCA framework, and the impact of DHN constructions on the environmental performance of geothermal district heating.

2. Kirchstockach geothermal power plant

2.1. Kirchstockach plant – reference case

The geothermal plant of Kirchstockach is considered as reference case for a binary system using a hydrothermal resource from a deep sedimentary basin. The plant is located south-east of Munich (Germany), where a geothermal resource is exploited with a mass flow rate of 432 m^3/h and an average production temperature of 138 °C (Table 1). At Kirchstockach, a two-stage ORC concept with a nominal electric capacity of 5.5 MW_{el} is realized. The plant has been in operation since 2013 and has originally been designed for pure electricity generation. Two separate ORC-modules are applied, both using the working fluid 1,1,1,3,3-Pentafluoropropane (R245fa). An overview of the technical concept and a thermodynamic analysis at design conditions is provided in Heberle et al. [11], and a comprehensive LCA of the plant in case of electricity generation only was conducted by Menberg et al. [37]. The technical realization of the Kirchstockach plant enables a retrofit by an

Table 1
Main characteristics of the geothermal plant in Kirchstockach considered for the LCA in this study for the reference case (pure electricity generation).

	Parameter	Value	Unit	Source
Subsurface	Overall borehole length	8,664	m	Operator data (SWM[a])
	Overall length of casing	13,200	m	Operator data (SWM[a])
	Drilling days	182	d	Operator data (SWM[a])
	Brine flow rate	432	m^3/h	Heberle et al. [11]
	Brine temperature	138	°C	Heberle et al. [11]
	Power demand downhole pumps	830	kW	Irl et al. [38]
Surface	Installed power capacity	5.5	MW_{el}	Heberle et al. [11]
	Power need ORC	788	kW	Eller et al. [42,43]
	ORC refrigerant R245fa	70,000	kg	Operator data (SWM[a])
Operation	Load hours	7,896	h/a	Bonafin et al. [39]
	Lifetime	30	a	Frick et al. [5], Parisi et al. [44]
	Annual refrigerant leakage rate	1	%	Operator data (SWM[a])

[a] SWM is the Stadtwerke München and the operator of the plant.

additional extraction of geothermal heat to a district heating network (DHN). For assessing the environmental effects of this option that is currently discussed in practice, the LCA is extended by selected cogeneration concepts. Additionally, the original case as studied in Menberg et al. [37] is refined according to the following main components, and a reference case is defined (Table 1).

- The power consumption of the borehole pump is specified according to recently published site-specific data [38]. This replaces previously estimated consumption data.
- The yearly operational hours of the power plant are set to 7,896 h/a according to Bonafin et al. [39], where a total availability of 90.1% for the Kirchstockach plant (including downhole pump and balance of plant) is reported. The average availability of the ORC system is therefore 98.1%.
- The production process of R245fa is specifically considered according to McCulloch [40], instead of using surrogate values for R134a. For leakage during the production process, supplementary data by Baral et al. [41] is incorporated, describing the production of R245fa as a side product.

2.2. Potential cogeneration concepts for Kirchstockach

The identification of suitable concepts for CHP generation under technical and thermodynamic criteria has been addressed in previous work. With focus on low-grade resources, parallel as well as serial configurations of binary unit and heat extraction are particularly of interest. Heberle and Brüggemann [45] analyzed these options under exergetic aspects. Thereby, the highest second law efficiency is obtained by a series configuration in combination with the ORC working fluid isopentane. With respect to high supply temperatures for conventional heating networks or industrial applications, Fiaschi et al. [46] propose a Cross Parallel CHP scheme in order to realise the heat supply on a temperature level of 80–140 °C. Van Erdeweghe et al. [47] analyzed several design concepts under thermo-economic criteria. Generally, that study proves a significant increase of net present value by applying a CHP concept compared to pure electricity generation. In this case, a series configuration leads to the highest cost-efficiency under the selected boundary conditions. Concerning a higher flexibility and part-load efficiency, Eyerer et al. [48] demonstrated an innovative approach by applying a two-stage concept with turbine bleeding and a regenerative direct contact preheater. This CHP concept was realized in a small-scale test rig and investigated under varying heat loads towards a minimum ORC load of 15.3%.

The existing geothermal power plant of Kirchstockach consists of a high-temperature (HT) and a low-temperature (LT) ORC unit. First, the brine is coupled to the HT-evaporator, the HHT-preheater, and in the following to the LT-evaporator. Finally, the geothermal fluid is split and led to the LT- and HT-preheater. Both ORC units utilize the same working fluid (R245fa) and for each, an air-cooled condenser is applied. Although the two-stage approach leads to a complex technical solution with a large number of components, the efficiency is increased compared to a classical one-stage concept with the same working fluid [11]. Furthermore, the flexibility and variety regarding potential cogeneration concepts is enhanced. In Fig. 1, three promising cogeneration architectures are illustrated: parallel, parallel-HHT, and LT concepts. Eller et al. [42] and Eller et al. [43] investigated these CHP architectures by deriving annual thermal load profiles typical for a location in Germany and performing dynamic modelling of the cogeneration concepts based on enthalpy and mass flow.

However, environmental issues have not been included in the analyses yet. Still, these studies identify the parallel-HHT concept as the most suitable design. Compared to pure electricity generation, an increase in second law efficiency of 4.9% and a 16.9% higher annual return is obtained in case of a DHN with 5 MW thermal peak load [42]. The developed methods and models, as well as the corresponding outputs of Eller et al. [42], are applied to this work in order to predict electrical and thermal outputs for a reliable LCI of the considered energy system.

2.3. District heating network

The two-stage ORC is extended by an additional heat extraction to a CHP system with a peak load of 10 MW_{th} thermal power (Table 2). The structure and geographical extension of the DHN are derived from the potential route plan shown in Fig. 2, considering all relevant settlement areas and industrial zones nearby the Kirchstockach power plant.

The required components, like a heat exchanger, a gas boiler and DHN pumps are located in a heating station with a building floor area of

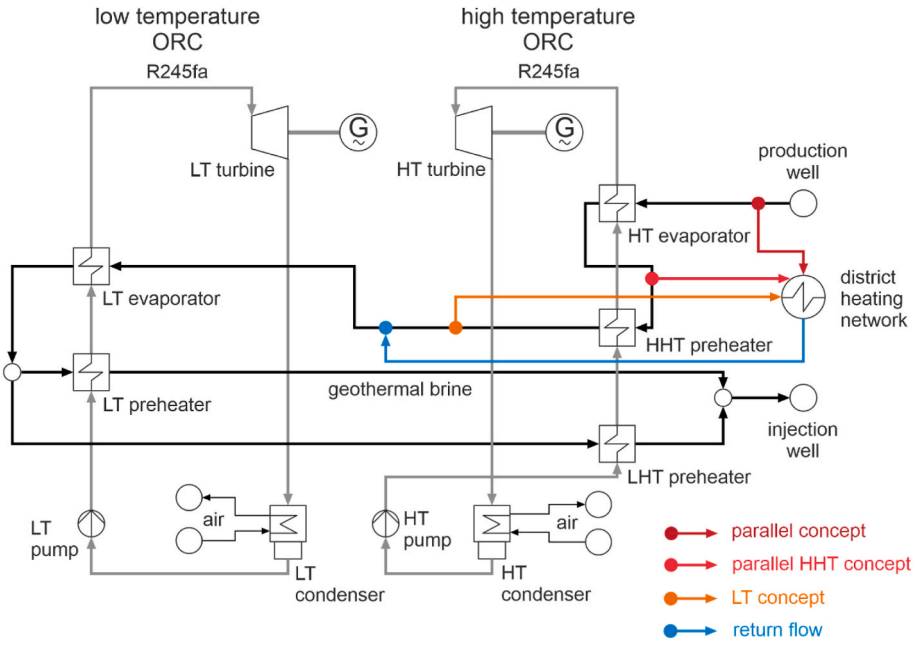

Fig. 1. Technical scheme of the two-stage ORC system in Kirchstockach. Coloured arrows indicate the investigated concepts of this study for additional heat extraction and supply to a DHN (modified from Menberg et al. [37]).

Table 2
Assumed Kirchstockach CHP plant characteristics used for the LCA, and shared by the investigated CHP concepts, based on Eller et al. [42,43].

Parameter	Value	Unit
Installed heat capacity	10	MW_{th}
Full load hours heat production	3,897	h/a
Provided heat[a]	35,069	MWh_{th}/a
Flow rate heat extraction	113.8	m^3/h
DHN supply temperature	90	°C
DHN return temperature	60	°C
DHN peak flow rate	293	m^3/h
Power demand of DHN pumps	293	kW

[a] Assuming 10% loss of generated heat (see Table 1) [42,43].

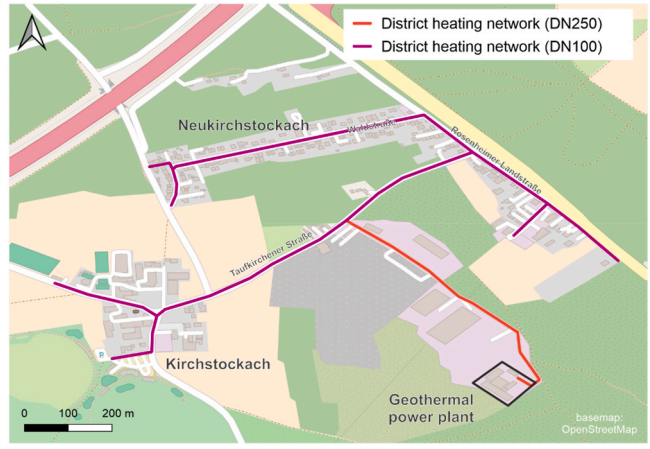

Fig. 2. Hypothetical DHN in Kirchstockach showing the main (diameter DN 250 mm) and intermediate heating grid (diameter DN 100 mm) with an overall length of 4,000 m. Exact locations of the smaller connection grid are not shown, but estimated per heat customer (see Table 4).

200 m^2. Heat transfer from the brine to the DHN is realized by a plate heat exchanger manufactured of high-alloyed steel (1.9 kg/kW_{th}). To ensure redundancy, a gas boiler is implemented, whereby only the installation and no operational hours are considered in the LCI. Due to reliability aspects, three DHN pumps with a specific power consumption of 1 $kW_{el}/(m^3/h)$ are implemented. For the piping in the heating station, 50 m of high-alloyed and 150 m of low-alloyed steel pipes are assumed. The detailed LCI of the built-in components is listed in the tables provided in Appendices A.3 – A.6.

Based on the notional map for the DHN in Fig. 2, main distribution pipes with a nominal diameter of 250 mm (DN 250) and 100 mm (DN 100) are assumed. For the investigated setup, the DHN would consist of 100 customers, including 92 residential transfer stations with a thermal capacity of 65 kW_{th}, as well as 8 transfer stations with industrial background and a thermal capacity of 390 kW_{th}. The connection between the customers and the main distribution pipes is assumed to be realized with DN 32 and DN 60 pipes, respectively. In case of residential units, the length of the subdistribution pipes is set to 25 m/unit and for industrial

Table 3
Characteristics of the hypothetical district heating network based on the geographical setting (Fig. 2).

Parameter	Value	Unit
Length main heating grid (diameter 250 mm)	1,000	m
Length intermediate heating grid (diameter 100 mm)	3,000	m
Length connection pipes (diameter 50 mm)	480[a]	m
Length connection pipes (diameter 32 mm)	2,300[b]	m
Number of household customers (65 kW_{th})	92	–
Number of industrial customers (390 kW_{th})	8	–

[a] Assuming 60 m per customer with 390 kW_{th}.
[b] Assuming 25 m per customer with 65 kW_{th}.

Table 4
Scenario-specific parameter values for power production under the different heat extraction concepts (see Fig. 1, based on Eller et al. [42,43]).

Concept	Parameter	Value	Unit
Reference	Gross power production	43,761	MWh_{el}/a
	Net power production	30,985	MWh_{el}/a
Parallel	Gross power production	38,534	MWh_{el}/a
	Net power production	24,617	MWh_{el}/a
Parallel HHT	Gross power production	39,993	MWh_{el}/a
	Net power production	26,076	MWh_{el}/a
LT	Gross power production	39,710	MWh_{el}/a
	Net power production	25,793	MWh_{el}/a

applications to 60 m/unit. In sum, a length of 6,780 m results for the DHN. In this context, the DHN Kirchstockach can be characterized by a connection density of 1.47 kW_{th}/m, which agrees to existing geothermal DHN in the Southern-German Molasse Basin, like Unterhaching (1.45 kW_{th}/m) or Poing (1.43 kW_{th}/m) [49,50]. In Table 3, all lengths of the DHN subsections and customers' information are listed.

In general, plastic casing pipes are considered for main pipes and connection pipes. They consist of a low-alloyed steel pipe, a polyurethane foam isolation and polyethylene casing. Details concerning the LCI of the production, transport and laying are given in Appendix A.3 and A.4. Underground pipes and demineralized water as heat transfer medium in the DHN are assumed. The LCI of heat transfer stations with the customers includes piping, armatures, plate heat exchangers, isolation, and electric wiring (see Appendix A.4).

2.4. Input data of the geothermal systems for the LCI

The yearly generated amount of electricity of the ORC system is calculated by the transient model of Eller et al. [42], which is validated with real power plant data of Kirchstockach. In particular, semi-empirical submodels for the ORC heat exchangers and rotating equipment are implemented. Therefore, the model is able to describe part load and off-design conditions of the entire ORC system depending on heat demand and ambient temperature. In comparison to the thermo-economic analysis by Eller et al. [42], the simulation of pure electricity is adapted according to the updated load hours (Table 1).

In case of cogeneration, the required heat demand profiles are developed from operational data of a geothermal heat plant as described by Eller et al. [42]. Incorrect data points are excluded and representative load profiles are associated to typical day categories defined by VDI 4655 [51]. Subsequently, the data set is weather-adjusted using degree days according to VDI 3807 [52], whereas the adjusted thermal energy consumption Q_{therm_a} is calculated by equation (1):

$$Q_{therm\_a} = Q_{therm\_na}\frac{G_{15m}}{G_{15}} \tag{1}$$

Thereby, the unadjusted thermal energy consumption of the reference year Q_{therm_na} is multiplied with the adjustment factor made up by the degree days for each typical day category for a long-term average G_{15m} in relation to the reference year G_{15} using weather data from 2016 [53]. In this respect, the degree days are determined according to VDI 4655 [51] based on equation (2):

$$G_{15} = \sum_{n=1}^{z}(20°C - t_{m,n}) \tag{2}$$

Here, $t_{m,n}$, as adapted by Eller et al. [42], is the mean ambient temperature over seven days for z days with $t_{m,n} < 15°C$. Additionally, the data is adopted to the peak load defined in Table 1. Finally, annual simulations are conducted.

The entire thermal energy demand is covered by the geothermal resource, considering averaged overall heat losses of 10%. This leads to an amount of supplied thermal energy of 35,069 MWh_{th}/a for all

considered CHP concepts. For the amount of electricity, a distinction between gross and net production is important. In Table 4, the relevant values are listed for the analyzed concepts. The reference case is related to pure power generation and updated from Menberg et al. [37] with the detailed LCI given in Table A.1. Therefore, the net electricity production considers auxiliary power requirements of the ORC feed pump and condenser fans as well as downhole pumps. For the CHP concepts, the electricity consumption of DHN feed pumps is additionally included.

3. Life cycle assessment

Details of the LCA application in this study are described in the following chapters according to the normed methodology in line with the standards ISO 14040 and 14044 [54,55]. First, goal and scope of the LCA are described, including the definition of the functional unit, for which all resource uses and emissions are identified, and the allocation schemes are discussed for those geothermal plant concepts with cogeneration of power and heat. Then, a comprehensive LCI is created, considering the specific components needed for the different CHP concepts and the DHN. For the LCIA, the IMPACT 2002+ [56] scheme is applied and environmental impacts of four midpoint categories, namely global warming (GWP, g_{eq} CO_2 into air), aquatic acidification (AP, mg_{eq} SO_2 into air) and eutrophication (EP, mg_{eq} PO_4^{3-} into water), and primary energy demand (MJ total primary non-renewable energy), are evaluated. This ensures consistent interpretation and comparability with previous studies on the Kirchstockach power plant [37].

3.1. Definition of goal and scope

The functional unit of this LCA is 1 kWh of electricity for the reference scenario, which considers only power generation. For assessment of the CHP concepts, both 1 kWh of electricity and 1 kWh of heat are considered by applying an allocation scheme based on the exergy content of the produced energy, as described by Frick et al. [5]. Here, allocation factors for power f_{el} and heat f_{th} are calculated based on equations (3) and (4) [5]:

$$f_{el} = \frac{Q_{el} w_{el}}{Q_{el} w_{el} + Q_{th} w_{th}} \tag{3}$$

$$f_{th} = \frac{Q_{th} w_{th}}{Q_{el} w_{el} + Q_{th} w_{th}} \tag{4}$$

with Q_{el} and Q_{th} representing the total amount of provided power and heat, respectively. w_{el} is the exergy content of power ($w_{el} = 1$), and w_{th} is the exergy content of heat, depending on the ambient temperature, T_a, the supply temperature of the DHN, T_{sup}, and its return temperature, T_{re} [5], as shown in equation (5):

$$w_{th} = 1 - T_a \frac{\ln\left(T_{sup}/T_{re}\right)}{T_{sup} - T_{re}} \tag{5}$$

The assumption of this exergy-based allocation scheme is in line with the recommendations of Parisi et al. [44], who suggest using this approach for a share of the coproduct (i.e., heat) of less than 75%. The different CHP concepts in our study exhibit shares between 73 and 78%. Further, the allocation scheme is assigned to impacts from components, which are used for power as well as heat production (geothermal wells, etc.), while components that are used for either power (e.g., ORC components) or heat (e.g., heat exchangers) production are fully allocated to their corresponding output.

We adopt the suggested lifetime of 30 years for both the power plant and the CHP concepts [44], which is also consistent with previous studies [5,37] (Table 1). System boundaries for electricity generation are set similar to most existing studies by not including the distribution via an electricity grid [5,8,37,44] (Fig. 3). In case of the CHP concepts, we explicitly account for the construction and operation of a DHN in Kirchstockach. As smaller town and villages in Germany typically either have a decentralised (oil, biomass, heat pumps, etc.) or a centralised heat supply by natural gas, the construction of a DHN is representative for many newly built geothermal plants outside large urban areas. Considering current trends in the Central European heating market, strategies for realizing a gas phase-out in the heating sector are discussed. This raises attention towards geothermal and low-temperature DHNs not only in new settlements but also as an alternative for heat supply in existing districts. Therefore, the results of this case study provide insights into environmental impacts of this transition in general.

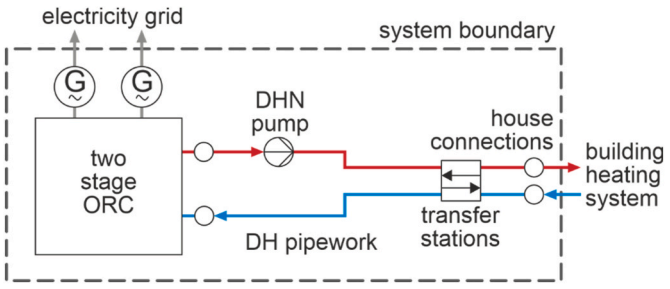

Fig. 3. System boundaries (dashed lines) for the combined power and heat generation LCA. For details of the two stage ORC see Fig. 1.

In terms of life cycle stages, the scope follows a cradle-to-grave approach by including the construction, operation and decommissioning (end-of-life) phase (Fig. 3). Auxiliary energy consumption during construction, i.e., electricity needed for geothermal well drilling, is assumed to be supplied by the German grid, while power demands during the operation phase for driving downhole pumps, ORC pumps, etc. are subtracted directly from the power output of the plant.

3.2. Life cycle inventory analysis

Following the workflows and recommendations of previous studies, we use site-specific data for the LCI of the Kirchstockach plant where possible [37,44], and resort to more general, Germany-wide data in cases where site-specific data is not available [5] (see Table A.1). For a detailed description of the LCI of the existing geothermal power plant in Kirchstockach, the reader is referred to Menberg et al. [37], as this is used as reference case for the present study. One adaptation to the previously used LCI is the consideration of specific background processes for the ORC working fluid R245fa used in Kirchstockach. As the loss of 1% of working fluid (see Table 1) plays a significant role for the global warming potential of the plant [37], a new comprehensive LCI for the production of one ton of R245fa (Table A.2) is introduced for this component.

For the assessment of CHP concepts, it is assumed that the additional components are located within an expanded (additional 200 m^2, ca. 30%) building of the geothermal power plant. Likewise, materials and processes for the additional heat exchangers, pipework, DHN pumps, etc. at the plant are added to the LCI (Table 5). Regarding the distribution of heat, construction materials and processes are considered according to the specific diameter and length of the hypothetical DHN (Fig. 2), as well as the number of customers given in Table 3 (Table A.3). Furthermore, one heat transfer station per costumer, as well as additional in-house pipework is included there. Detailed LCIs for the construction of DHN sections for different diameters, transfer stations and house connections are provided in Appendices A.4 - A.6. If not indicated otherwise, all materials and processes are adopted from Ecoinvent 3.5 using the "allocation, cut-off by classification" scheme [57].

4. Impact assessment and interpretation

4.1. Kirchstockach reference case and CHP scenarios

Fig. 4 shows the LCA results for the reference case (electricity

Table 5
LCI showing the site-specific data of the Kirchstockach CHP plant. LCI data on further components is adopted from Menberg et al. [37] and listed in the Appendix.

	Component	Material	Amount	Uncertainty
Plant building[a]		Concrete, sole plate and foundation (CH)	1,677 m^3	±5%
		Steel, unalloyed (GLO)	1,625 kg	±5%
		Transport, freight, lorry >32 metric ton, euro4 (RER)	65 tkm	±5%
		Transport, freight train 8Europe without Switzerland)	65 tkm	±5%
		Diesel, burned in building machine (GLO)	1,300 MJ	±5%
CHP unit[b]	Plate heat exchanger	Steel, chromium steel 18/8 (GLO)	19,000 kg	±10%
	DHN pumps	Steel, low-alloyed (GLO)	9,757 kg	±5%
	Gas Boiler	Steel, low-alloyed (GLO)	16,500 kg	±10%
	Pipework brine	Steel, chromium steel 18/8 (GLO)	2,276 kg	±5%
		Rock wool, packed (GLO)	1,423 kg	±5%
	Pipework DHN	Steel, low-alloyed (GLO)	5,121 kg	±5%
		Rock wool, packed (GLO)	1,707 kg	±5%
	Transport	Transport, freight, lorry >32 metric ton, euro5 (RER)	11,157 tkm	±5%

[a] Based on data from Frick et al. [5] plus 20% accounting for the additional space requirements of the CHP unit.
[b] Based on own calculations accounting for site-specific characteristics and capacities.

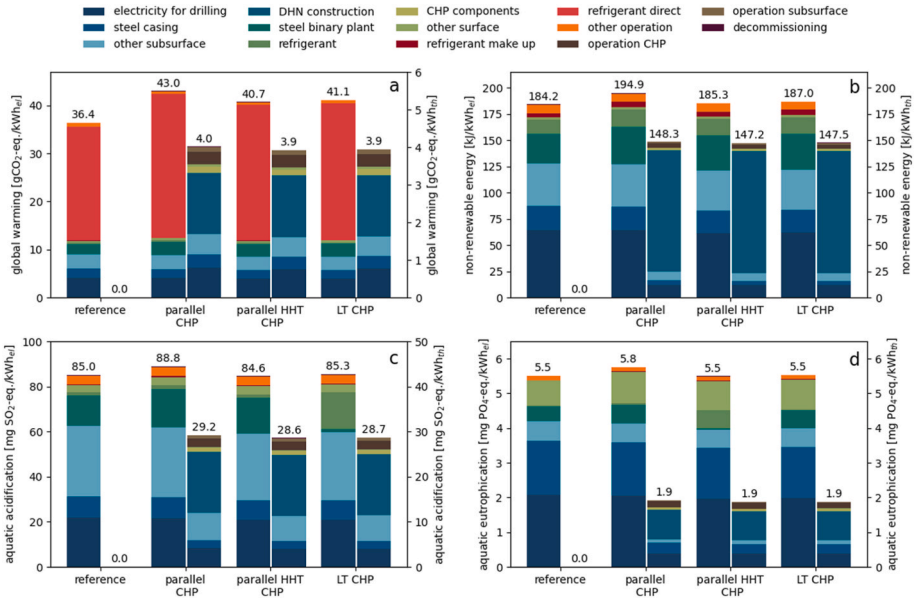

Fig. 4. LCA results for the Kirchstockach reference case (no cogeneration), and the three investigated cogeneration concepts with exergy-based allocation between electricity (left bar plot/y-axis) and heat output (right bar plot/y-axis); a) to d) show four different environmental impact categories. Note the difference in scale of emissions per kWh_{th} (right y-axis) in a) and c).

production only) and the three cogeneration concepts (parallel, parallel HHT and LT CHP, see Fig. 1), for which further differentiation of environmental impact per generated kWh electricity (kWh_{el}, left-hand bars) and heat (kWh_{th}, right-hand bars) is introduced. Accordingly, there is no impact per kWh_{th} for the reference case.

A comparison of the reference case and the considered cogeneration concepts shows a slight increase in environmental impacts for electricity generation in the CHP scenarios, which is expected as part of the extracted geothermal heat is used for heat generation instead (Table 4). Also, the auxiliary energy demand for the CHP components is supplied by the ORC, leading to a reduction of net power output. This effect depends on the allocation method of auxiliary power demand in the LCA, which will be further investigated below. Overall, only minor differences result between the considered cogeneration concepts within each impact category in terms of magnitude of individual environmental impacts, as well as regarding the contribution of different life-cycle stages, components, etc. to the overall emissions (Fig. 4). However, there are some significant differences between the impact categories regarding the amount of emissions being associated with power (kWh_{el}) and heat (kWh_{th}) output.

The global warming potential (GWP) of geothermal district heating is one order of magnitude lower than for electricity generation, regardless of the adopted cogeneration option. As the direct emissions of the ORC refrigerant are fully allocated to the electricity output, the main contributors to greenhouse gas (GHG) emissions for district heating are the allocated emissions of the subsurface construction (well drilling, steel casing, etc.) and the DHN construction in particular. These amount up to 40% of the GWP, yet the absolute emissions are low with 1.6 gCO_2-eq./kWh_{th}. In contrast, the impact of district heating in terms of non-renewable energy demand is within the same order of magnitude as for electricity generation. This is mainly caused by the high energy demand during the construction phase of the DHN, dominated by diesel-driven construction machines and asphalt needed for road works (116 kJ/kWh_{th}, 78%). The aquatic acidification and eutrophication potential of district heating amount up to roughly a third of those for electricity generation, and are again mostly caused by the construction of the DHN (AP: 44%, EP: 48%) and the subsurface components of the geothermal plant (AP: 40%, EP: 42%).

In the following, results from Kirchstockach are compared to previous studies with a focus on environmental emissions from geothermal cogeneration. For a more comprehensive discussion of the burdens of electricity output, the reader is referred to Menberg et al. [37]. LCA of the Hellisheiði CHP plant revealed emissions of approx. 20 gCO_2-eq./kWh_{el} and 5.5 gCO_2-eq./kWh_{th} using an exergy-based allocation [58], which are in the same order of magnitude as in

Kirchstockach. Emissions from an energy-based allocation for the same CHP plant yielded slightly lower emissions for the impact categories of GWP, EP and AP, which are to be attributed to the different type of geothermal resource and much larger capacity (303 MW_{el}, 200 MW_{th}), as well as the difference in allocation factors (92% exergy, 8% heat) [12]. The non-renewable energy demand, however, is several orders of magnitude lower for the Hellisheiði CHP plant, even when accounting for the DHN construction considered in the present study, which is linked to the low amount of fossil fuels being used in Hellisheiði [12]. For an Enhanced Geothermal System CHP plant in Illkirch in the Upper Rhine Valley, that has a similar capacity as Kirchstockach, very similar values close to 50 gCO_2-eq./kWh_{el} and less than 5 gCO_2-eq./kWh_{th} were reported, with geothermal well and ORC construction causing the highest shares of emissions [27]. For hypothetical German binary power plant setups, Frick et al. [5] also obtained lower impacts for CHP plants than for pure electricity output. However, only relative emissions with respect to the past heating and electricity mix are given and impede detailed comparison.

Compared to a previous assessment of the Kirchstockach power plant, the LCA results for the reference case of this study show slightly lower emissions for the four main impact categories than compared to the results in Menberg et al. [37]. This is partly due to the increased net power production stemming from a higher number of annual load hours (Table 4), although this increase is to some extent compensated by higher auxiliary power demands (Table 1). Also, the newly modelled environmental emissions for production of R245fa are lower than those of R134a, available in Ecoinvent 3.5 [57]. An inspection of background processes and materials reveals that the energy input for the production of both refrigerants is similar, yet the use of tetrachloroethylene and trichloroethylene in Ecoinvent for the production of R134a has a significantly higher impact than the substance used for R245fa (Table A.2). Also, it can be assumed that the by-product of hydrochloric acid is re-used and therefore the environmental impact of the production of hydrochloric acid can be subtracted, which reduces the CO_2 emissions by around 60% in comparison to ignoring re-use.

In terms of GHG emissions, cogeneration of heat in Kirchstockach would outperform most other heating technologies in Germany. Fossil fuel-based systems, such as heating oil, natural gas, and district heating on average emit around 319, 251, and 229 gCO_2-eq./kW_{th}, respectively [59]. Also, shallow geothermal systems, such as aquifer thermal energy storage and ground-source heat pump systems, were shown to have higher GHG emissions in the range of 83–120 and 98–156 gCO_2-eq./kW_{th}, respectively, due the high auxiliary electricity demand of the heat pumps used [23,25,60–63].

4.2. Auxiliary energy demand for power and heat production

Besides the choice of allocation factor (energy, exergy, etc.), the scheme of individual process and material allocation to the corresponding outputs (heat and/or electricity) can influence the LCA outputs of cogeneration plants [37,58,64]. Thus, this section examines different allocation and supply schemes in terms of assigning the burdens of the auxiliary energy consumed for the CHP plant. In the previous chapter, the results using the most common scheme were discussed, in which auxiliary energy demand for CHP components is supplied by the ORC (i.e., the life-time power output of the ORC power is decreased accordingly), yet the corresponding emissions are not allocated with the generated heat output (i.e., full allocation to electricity). For this, an additional scheme is defined, in which the environmental burden of the decreased net power output is allocated with the heat output according to the chosen exergy-based approach. A third scheme goes one step further and assumes a supply of auxiliary energy demand of the ORC and the CHP components (e.g., DHN pumps) directly from the German grid. In that sense, this scheme represents the worst case in terms of assigning embedded emissions from auxiliary energy to the CHP outputs.

The results for the three allocation schemes (allocation of auxiliary energy to electricity/electricity and heat, and supply from grid) are shown in Fig. 5 for the low-temperature (LT) CHP concept with medium emissions (see Fig. 4). It reveals that the common scheme, with no allocation of embedded emissions from auxiliary energy, environmentally favours heat production. Yet, even when the burdens from auxiliary energy demand are allocated with both outputs, the shift of emissions from electricity to heat production is only minor. In contrast, as expected, the scheme with supply from the German grid shows the highest emissions. This scheme also allows to further assess the influence of individual auxiliary power demands on the environmental performance of the CHP plant. While emissions related to electricity output are dominated by the power demand of the ORC and the downhole pump, the impact for heat production is almost equally distributed between the allocated share of the power demand of the downhole pump and the pump of the DHN (Fig. 5). Obviously, the absolute values for in this scheme depend on the environmental burden of the chosen electricity mix (in this study the German electricity mix of 2018 with 470 gCO_2-eq./kWh [65]), while the relative pattern of increased emissions will be the same for every carbon-intensive grid mix. However, even when supplying the auxiliary energy demand from the German grid, GHG emissions for cogeneration of heat are still significantly lower than for most common technologies (see previous chapter).

The effects of different allocation methods and factors were also shown to have a significant impact on the environmental impact of geothermal cogeneration for the Hellisheiði CHP plant: Karlsdottir et al. [58] reported a variation of 25% in the GHG emissions for electricity generation, and of 95% for heat generation, when different allocation methods are applied (e.g., energy-based, exergy-based, etc.). The variation in the LCA results in Fig. 5 reveals that GHG emissions from the CHP plant of Kirchstockach are also sensitive to the way how auxiliary energy needs are assigned to the generated power.

4.3. Impacts of district heating network

As the overall LCA results reveal that the environmental burden of generated heat is dominated by the construction of the DHN (Fig. 4), this section is included to analyse two more setups for the DHN in Kirchstockach. While the originally proposed setup (Fig. 2) corresponds to a newly installed DHN mostly under road surfaces in an built-up area, the first alternative setup (“DHN grass”) assumes that the main heating grid (DN 250), as well as two third (i.e., 2,000 m) of the intermediate heating grid (DN 100) are installed not below, but next to roads in grass-covered subsurface. The second alternative (“DHN short”) represents a setup where, as in many German cities, a DHN is pre-existing and the conventional energy source (e.g., gas-fired CHP plant) is substituted by geothermal heat supply. In this case, only a main heating grid connection of 1,000 m with DN 250 would be required to connect the CHP plant (Fig. 2).

The results for the three different DHN setups (original LT CHP concept, under grass and short) and the corresponding uncertainties are shown in Fig. 6 for the LT CHP concept, following the scheme with no allocation for the auxiliary power demand. As the emissions of DHN construction are fully allocated with the generated heat, only emissions per kWh_{th} are shown, including output ranges that arise from the parameter uncertainties in the LCI (Appendices A.1 – A.6). The installation of DHN pipes under grass-covered surfaces avoids environmental impacts from asphalt production and processing, so that the setup “DHN grass” shows a significantly lower non-renewable energy demand than the original LT CHP concept. For the other impact categories, only minor changes are observed for this scenario, and a further reduction in emissions in the setup of a short DHN connection (Fig. 6). However, the non-renewable energy demand is again slightly higher for the shorter DHN under road surfaces, which again highlights the significant non-renewable energy demand of road constructions work included in the LCI in this study. Fig. 6 shows that relative uncertainties are also significantly higher for the non-renewable energy demand (±19–30%) and in particular for the eutrophication potential (±50–240%), than for global warming (±8–14%) and acidification potential (±11–23%).

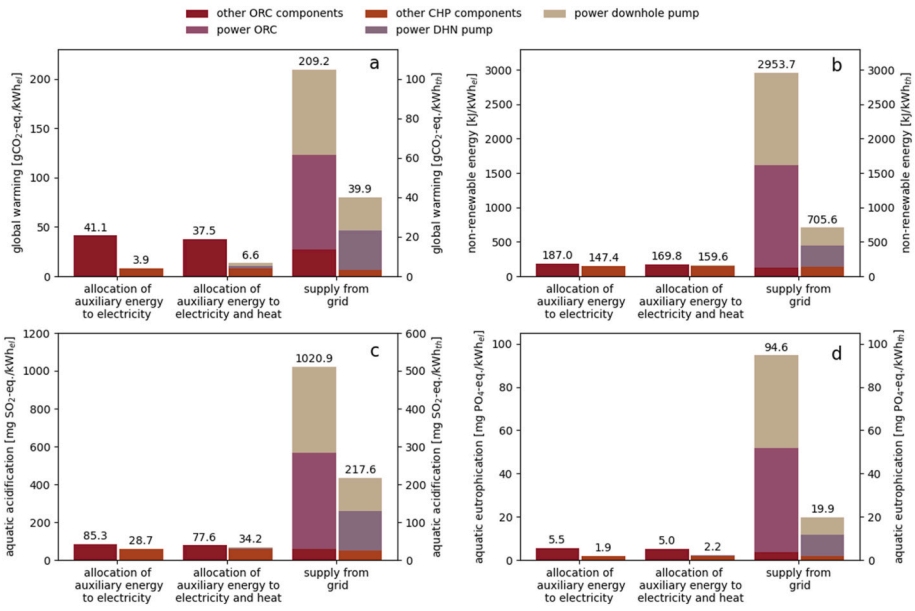

Fig. 5. LCA results for the low temperature (LT) combined heat and power concept in Kirchstockach for varying allocation and supply schemes regarding the environmental burden of auxiliary electricity. Each scheme is assessed with respect to electricity (left bar plot/y-axis) and heat generation (right bar plot/y-axis). Results are shown for four impact categories (a–d). Note the difference in scale between emissions per kWh_{el} and kWh_{th} in a) and c).

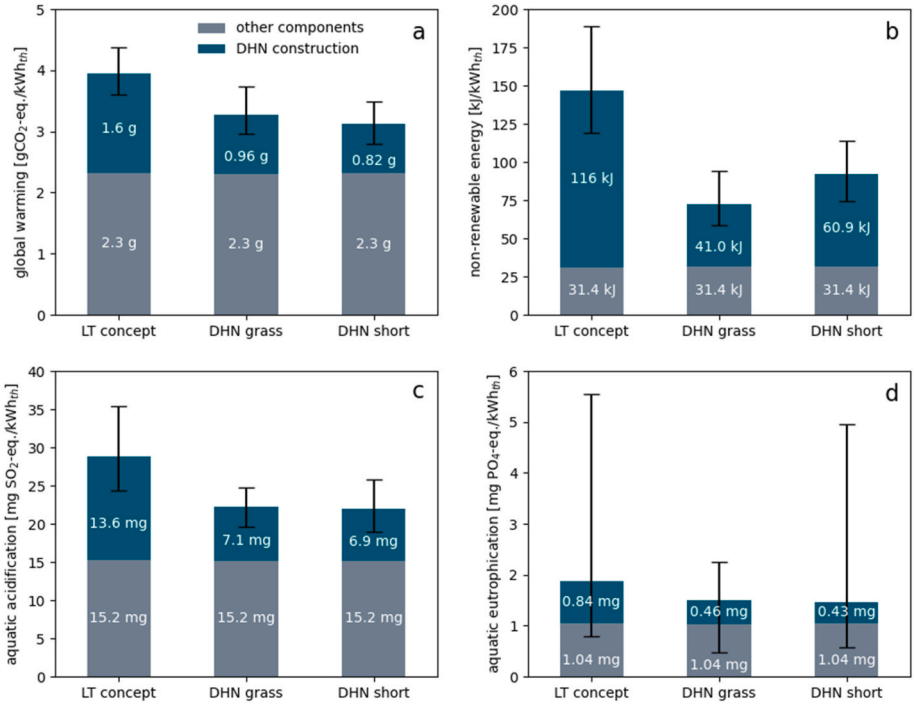

Fig. 6. LCA results for the LT CHP concept, with a DHN setup partially under grass surface and a shorter network of 1 km length. Results are shown for four impact categories (a–d) and heat output only (kWh_{th}). Uncertainties shown are based on Monte Carlo simulation using the values in Appendices A.1 – A.6.

5. Conclusions

In this study, a comprehensive life-cycle assessment (LCA) of a hydrothermal plant with different technical concepts for cogeneration of power and heat is presented. While there is currently no combined heat and power (CHP) concept in place at the analyzed system of Kirchstockach, the life-cycle inventory (LCI) for power generation is based on actual plant data. This LCI is extended to encompass the construction of a CHP plant, including a hypothetical district heating network (DHN), as well as detailed background data for the refrigerant R245fa, which is used in the Organic Ranking Cycle (ORC) in Kirchstockach.

The newly incorporated process for R245fa production requires similar inputs in terms of energy as R134a, which was used as a substitute in the LCI of a previous reference study. Yet, this leads to lower background emissions from production materials and reduces global warming potential (GWP) of R245fa and thus also the GWP of geothermal energy without CHP (36.4 gCO_2-eq./kWh_{el}). The different CHP concepts (parallel, parallel high temperature, low temperature concept) perform similarly well compared to conventional energy technologies in terms of GWP (40.7–43.0 gCO_2-eq./kWh_{el}), non-renewable energy demand (185.3–194.4 kJ/kWh_{el}), as well as eutrophication potential (84.6–88.8 mgSO_2-eq./kWh_{el}) and acidification

potential (5.5–5.8 $mgPO_4$-eq./kWh_{th}).

For generated heat, the environmental benefit is even larger, with GWPs being about two orders of magnitude lower (ca. 4 gCO_2-eq./kWh_{th}) than fossil fuel-based heating technologies, and also significantly larger than most shallow geothermal systems. However, the results show that the construction of a DHN can lead to high overall non-renewable energy demands due to diesel-driven construction machines and production of asphalt for construction under road surfaces. Accordingly, CHP concepts perform significantly better (up to 37% for non-renewable energy demand in Kirchstockach) in case of a pre-existing DHN, or when construction works are environmentally optimized.

A comparison of different allocation schemes for the environmental burden of auxiliary energy between the two outputs (i.e., power and heat) showed no significant variation in the resulting emissions, as long as the auxiliary energy is supplied by the ORC of the plant. Finally, an assessment of uncertainties in the environmental emissions revealed that these are highest for eutrophication potential and again non-renewable energy demand.

CRediT authorship contribution statement

Kathrin Menberg: Conceptualization, Formal analysis, Visualization, Writing – original draft. **Florian Heberle:** Investigation, Writing – original draft. **Hannah Uhrmann:** Investigation, Writing – review & editing. **Christoph Bott:** Writing – original draft. **Sebastian Grünäugl:** Investigation. **Dieter Brüggemann:** Writing – review & editing. **Peter Bayer:** Conceptualization, Writing – review & editing.

Declaration of competing interest

The authors declare that they have no known competing financial interests or personal relationships that could have appeared to influence the work reported in this paper.

Acknowledgements

The funding from the Bavarian State Ministry for Education, Science and the Arts in the framework of the project "Geothermie-Allianz Bayern", and the funding for Kathrin Menberg via the Margarete von Wrangell program of the Ministry of Science, Research and the Arts of the State of Baden-Württemberg are gratefully acknowledged. Furthermore, we would like to thank the operator of Kirchstockach power plant, Stadtwerke München GmbH (SWM), for the comprehensive provision of specific project data. Harry Keeton is acknowledged for his support with SimaPro LCA calculations.

Appendix

Table A.1
Complete LCI used for the reference case LCA of the Kirchstockach power plant, according to Menberg et al. [37] and references therein.

	Component	Material	Amount	Uncertainty[a]
Subsurface	Casing	Steel, low-alloyed	124.4 kg/m	±5%
	Cementation[b]	Bentonite, at processing	0.2 kg	±20%
		Chemicals inorganic, at plant	0.4 kg	±20%
		Portland calcareous cement, at plant	23.5 kg	±20%
		Silica sand, at plant	7 kg	±20%
		Cement, unspecified, at plant	7.3 kg	±20%
		Water, decarbonized, at plant	16.9 kg	±20%
	Drilling mud[b]	Chemicals inorganic, at plant	6.7 kg	±20%
		Bentonite, at processing	7.7 kg	±20%
		Potato starch, at plant	12.8 kg	±20%
		Lime, hydrated, packed, at plant	5.4 kg	±20%
		Calcareous marl, at plant/CH U	6.7 kg	±20%
		Water, decarbonized, at plant/RER U	671.4 kg	±20%
		Diesel, burned in diesel-electric generating set	181.3 kg	±20%
		Waste, from drilling, unspecified	456 kg	±5%
	Drilling energy	Electricity, medium voltage, at grid	2,630 MJ/m	±10%
	Reservoir enhancement[c]	Water, decarbonized, at plant	260,000 t	±40%
		Diesel, burned in diesel-electric generating set	3,000 GJ	±40%
	Transport[c]	Transport, lorry >32 t, EURO4	144,000 tkm	±20%
		Transport, freight, rail	413,000 tkm	±20%
	Drill site[d]	Diesel, burned in building machine	20,000 MJ	±5%
		Cement, unspecified, at plant	300 kg	±5%
	Geothermal fluid cycle[d]	Steel, low-alloyed, at plant	132,678 kg	±5%
		Diesel, burned in building machine	12,160 MJ	±5%
		Transport, lorry >32 t, EURO4	5,307 tkm	±5%
		Transport, freight, rail	53,734 tkm	±5%
surface	Heat exchanger	Steel, electric, chromium steel 18/8, at plant	87.6 t	±5%
	Air coolers LT & HT	Steel, electric, chromium steel 18/8, at plant	289.3 t	±5%
	ORC turbine	Steel, electric, chromium steel 18/8, at plant	13.7 t	±5%
	ORC pipes	Steel, electric, chromium steel 18/8, at plant	96.8 t	±5%
	ORC feed pump	Steel, electric, chromium steel 18/8, at plant	1.1 t	±5%
	Refrigerant	Refrigerant R254fa[e]	70,000 kg	fixed
	Binary unit[d]	Copper, at regional storage	6,600 kg	±10%
		Transport, freight, rail	2,000 tkm	±10%
		Transport, lorry >32 t, EURO5	50 tkm	±10%
	Plant building	Concrete, sole plate and foundation, at plant	1,290 m^3	±5%
		Diesel, burned in building machine	1,000 MJ	±5%
		Steel, low-alloyed, at plant[d]	1,250 kg	±5%
		Transport, lorry >32 t, EURO4[d]	50 tkm	±5%
		Transport, freight, rail[d]	50 tkm	±5%

(continued on next page)

Table A.1 (*continued*)

	Component	Material	Amount	Uncertainty[a]
Operation	Refrigerant[e]	Direct emissions from leaked fluid (GWP only)	1%	fixed
		Refrigerant R254fa[e]	1%	fixed
	Disposal filters[d]	Disposal, hazardous waste, 25% water, to hazardous waste incineration	21,060 kg	±20%
		Transport, lorry >32 t, EURO4	7,500 tkm	±20%
	Exchange downhole pump[d]	Steel, electric, chromium steel 18/8, at plant	135 t	±20%
		Disposal, steel, to municipal incineration	135 t	±20%
Decommissioning	Dismantling subsurface[d]	Gravel, unspecified, at mine	442,832 kg	±5%
		Cement, unspecified, at plant	42,463 kg	±5%
	Dismantling surface	Disposal, building, concrete, to final disposal	19.0 t	±5%
		Disposal, copper, to municipal incineration	13,200 kg	±5%
		Disposal, steel, to municipal incineration	265,356 kg	±5%
		Disposal, steel, to municipal incineration	415.8 kg	±5%
		Disposal, hazardous waste, 25% water, to hazardous waste incineration	3,300 kg	±5%

[a]n uncertainties for the specific materials and processes according to Frick et al. [5].
[b] values per meter well adopted from Frick et al. [5], material/process names according to ecoinvent 3.5.
[c] values per well, adopted from Frick et al. [5].
[d] overall values, adopted from Frick et al. [5].

Table A.2
LCI for the production of 1 ton of R245fa, based on information from McCulloch [40] and Baral et al. [41].

	Material/process	Amount	Uncertainty
Inputs	Water, deionised (RoW)	39 t	±5%
	Sodium chloride, powder (GLO)	3.1 t	±5%
	Fluorspar, 97% purity (GLO)	1.8 t	±5%
	Sulfur (GLO)	0.88 t	±5%
	Natural gas, high pressure (GLO)	2,200 m^3	±5%
	Base oil (GLO)	0.3 t	±5%
	Limestone, crushed, washed (GLO)	0.06 t	±5%
	Phosphate (GLO)	0.012 t	±5%
	Electricity, high voltage (GLO)	2.7 MWh	±5%
	Heat, district or industrial, natural gas (GLO)	33 GJ	±5%
	Heavy fuel oil, burned in refinery furnace (GLO)	0.01 GJ	±5%
	Transport, freight, lorry, unspecified (GLO)	1,481 tkm	±5%
Outputs to technosphere	Hydrochloric acid, without water, in 30% solution state (RoW)[a]	2.4 t	±5%
	Sodium chloride (emissions to water)	9.3 t	±5%
	Waste water treatment, chemical reduction/oxidation process, municipal waste water, at waste water treatment plant (RER)	30 t	±5%
	Sulfat (emissions to soil)	2.8 t	±5%
	Calcium (emissions to soil)	0.85 t	±5%
	Mineral waste, from mining (final waste flows)	1.8 t	±5%
	Sulfur dioxide (emissions to air)	5 kg	±5%
	VOC, volatile organic compounds, unspecified origin (emissions to air)	1 kg	±5%
	Propane, 1,1,1,3,3-pentafluoro-, HFC-245fa (emissions to air)	0.02913 kg	±5%

[a] considered as avoided product (i.e., produced for sale and further use).

Table A.3
Life cycle inventory (LCI) showing the type and number of individual components used in the DHN. For the LCI of the individual components see following tables A.4-A.6.

	Component	Amount	Uncertainty
Construction DHN	Heating grid section DN 250, under road	1,000 m	fixed
	Heating grid section DN 100, under road	3,000 m	fixed
	Heating grid section DN 50, under road[a]	96 m	fixed
	Heating grid section DN 50, under bare surface[b]	384 m	fixed
	Heating grid section DN 32, under road[b]	480 m	fixed
	Heating grid section DN 32, under bare surface[b]	1,840 m	fixed
	Transfer station 390 kW_{th}	8	fixed
	Transfer station 65 kW_{th}	92	fixed
	Customer connection 390 kW_{th}	8	fixed
	Customer connection 65 kW_{th}	92	fixed

[a] assuming 60 m per customer of 390 kW_{th}, with 20% of heating grid installed under road surface, 80% under bare surface (e.g., grass).
[b] assuming 25 m per customer of 65 kW_{th}, with 20% of heating grid installed under road surface, 80% under bare surface (e.g., grass).

Table A.4
Life cycle inventories (LCI) for 1 m of heating grid with different diameters (DN 32 – DN250) installed under an asphalt road. The LCI for a grid section under grassland is identical, except for bitumen and asphalt, which do not apply to there, and diesel use and transport, which are reduced accordingly.

Uncertainty		±5%	±5%	±5%	±5%	±5%	±5%	±5%	±5%	±5%	±5%	±5%	±5%	±5%	±5%
Amount	DN 32	6.19 kg	3.11 kg	1.78 kg	0.006 kg	0.011 kg	0.030 kg	0.032 kg	2.04 kg	572 kg	624 kg	342 kg	240 kg	2.16 MJ	258.4 MJ	36.3 tkm
	DN 50	9.01 kg	3.55 kg	2.21 kg	0.007 kg	0.011 kg	0.031 kg	0.033 kg	4.56 kg	592 kg	624 kg	342 kg	240 kg	2.25 MJ	289.6 MJ	37.06 tkm
	DN 100	19.66 kg	5.07 kg	3.8 kg	0.010 kg	0.011 kg	0.032 kg	0.034 kg	18.02 kg	1,139 kg	655 kg	360 kg	252 kg	2.3 MJ	318.1 MJ	50.63 tkm
	DN 250	66.09 kg	12.71 kg	8.56 kg	0.014 kg	0.028 kg	0.033 kg	0.036 kg	108.65 kg	1,755 kg	1,248 kg	684 kg	480 kg	2.4 MJ	590.2 MJ	92.54 tkm
Material/ process		Steel, low-alloyed (GLO)	Polyethylene, high density, granulate, recycled (Europe without Switzerland)	Polyurethane, rigid foam (RER)	Polyols, at plant (RER)[a]	Toluene diisocyanate (RER)	Argon, liquid (RER)	1-propanol (GLO)	Water, completely softened, from decarbonised water, at user (RER)	Sand (GLO)	Gravel, crushed (CH)	Bitumen adhesive compound, hot (GLO)	Disposal of asphalt[b]	Diesel, burned in diesel-electric generating set, 18.5 kW (GLO)	Diesel, burned in building machine (GLO)	Transport, freight, lorry >32 metric ton, euro5 (RER)

[a] process from Ecoinvent 2.2 [66].
[b] disposal scenario based on disposal of asphalt to sanitary landfill (CH) in Ecoinvent 2.2 [66].

Table A.5
Life cycle inventory per transfer station from grid to customer for different thermal capacities.

	Material/process	Amount	Uncertainty
DHN transfer station, 390kW$_{th}$	Steel, chromium steel 18/8 (GLO)	157.1 kg	±5%
	Polypropylene, granulate (GLO)	7.3 kg	±5%
	Copper (GLO)	1.9 kg	±5%
	Steel, low-alloyed (GLO)	245.7 kg	±5%
	Transport, freight, lorry >32 metric ton, euro5 (RER)	41.2 tkm	±5%
DHN transfer station, 65kW$_{th}$	Steel, chromium steel 18/8 (GLO)	20.9 kg	±5%
	Polypropylene, granulate (GLO)	2.6 kg	±5%
	Copper (GLO)	1.1 kg	±5%
	Steel, low-alloyed (GLO)	56.7 kg	±5%
	Transport, freight, lorry >32 metric ton, euro5 (RER)	8.1 tkm	±5%

Table A.6
Life cycle inventories for each heating grid customer connection for different capacities, including additionally required heating pipework.

	Material/process	Amount	Uncertainty
Pipework building, DN65	Steel, low-alloyed (GLO)	18.7 kg	±5%
	Rock wool, packed (GLO)	9.4 kg	±5%
	Transport, freight, lorry >32 metric ton, euro5 (RER)	2.8 tkm	±5%
Pipework building, DN32	Steel, low-alloyed (GLO)	8.8 kg	±5%
	Rock wool, packed (GLO)	2.47 kg	±5%
	Transport, freight, lorry >32 metric ton, euro5 (RER)	1.13 tkm	±5%
DHN customer connection, 390kW$_{th}$	Steel, low-alloyed (GLO)	14.0 kg	±5%
	Pipework building, DN65	15 pieces	fixed
	DHN transfer station, 390kW$_{th}$	1 piece	fixed
	Transport, freight, lorry >32 metric ton, euro5 (RER)	1.4 tkm	±5%
DHN customer connection, 65kW$_{th}$	Steel, low-alloyed (GLO)	6.8 kg	±5%
	Pipework building, DN32	12 pieces	fixed
	DHN transfer station, 65kW$_{th}$	1 piece	fixed
	Transport, freight, lorry >32 metric ton, euro5 (RER)	0.68 tkm	±5%

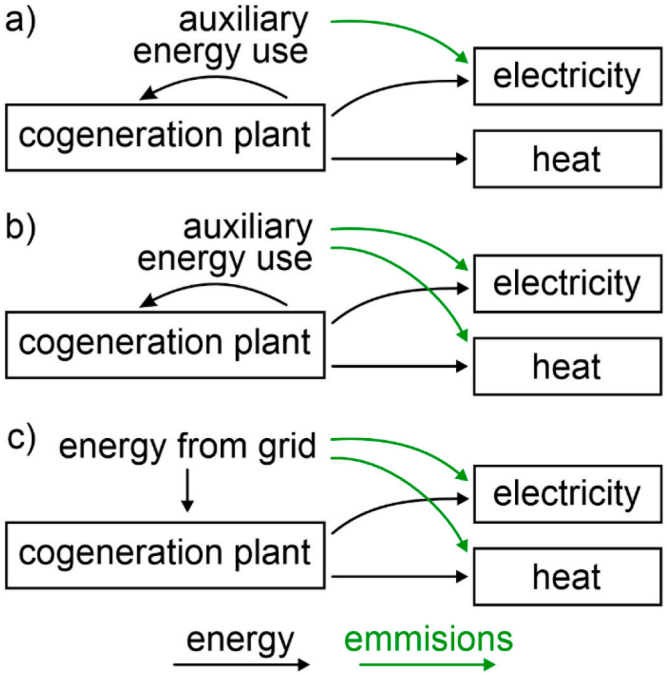

Fig. A.1. Graphical illustration of the three allocation schemes regarding the two outputs (electricity and heat) of the cogeneration plant, showing the corresponding energy flow (black) and allocation of background emissions (green) for a) allocation with self-supply of auxiliary energy, b) auxiliary energy with full allocation to both outputs, and c) supply of auxiliary energy from grid.

References

[1] P. Bayer, L. Rybach, P. Blum, R. Brauchler, Review on life cycle environmental effects of geothermal power generation, Renew. Sustain. Energy Rev. 26 (2013) 446–463.
[2] A. Eberle, G.A. Heath, A.C. Carpenter Petri, S.R. Nicholson, Systematic Review of Life Cycle Greenhouse Gas Emissions from Geothermal Electricity, 2017.
[3] M.L. Parisi, N. Ferrara, L. Torsello, R. Basosi, Life cycle assessment of atmospheric emission profiles of the Italian geothermal power plants, J. Clean. Prod. 234 (2019) 881–894.
[4] R. Basosi, R. Bonciani, D. Frosali, G. Manfrida, M.L. Parisi, F. Sansone, Life cycle analysis of a geothermal power plant: comparison of the environmental performance with other renewable energy systems, Sustainability 12 (7) (2020) 2786.
[5] S. Frick, M. Kaltschmitt, G. Schröder, Life cycle assessment of geothermal binary power plants using enhanced low-temperature reservoirs, Energy 35 (5) (2010) 2281–2294.
[6] F. Marty, S. Serra, S. Sochard, J.-M. Reneaume, Simultaneous optimization of the district heating network topology and the Organic Rankine Cycle sizing of a geothermal plant, Energy 159 (2018) 1060–1074.
[7] A.T. McCay, M.E. Feliks, J.J. Roberts, Life cycle assessment of the carbon intensity of deep geothermal heat systems: a case study from Scotland, Sci. Total Environ. 685 (2019) 208–219.
[8] K. Menberg, S. Pfister, P. Blum, P. Bayer, A matter of meters: state of the art in the life cycle assessment of enhanced geothermal systems, Energy Environ. Sci. 9 (9) (2016) 2720–2743.
[9] M. Lacirignola, I. Blanc, Environmental analysis of practical design options for enhanced geothermal systems (EGS) through life-cycle assessment, Renew. Energy 50 (2013) 901–914.
[10] Y. Ding, C. Liu, C. Zhang, X. Xu, Q. Li, L. Mao, Exergoenvironmental model of Organic Rankine Cycle system including the manufacture and leakage of working fluid, Energy 145 (2018) 52–64.
[11] F. Heberle, T. Jahrfeld, D. Brüggemann, Thermodynamic Analysis of Double-Stage Organic Rankine Cycles for Low-Enthalpy Sources Based on a Case Study for 5.5 MWe Power Plant Kirchstockach (Germany), Proceedings of the World Geothermal Congress, Melbourne, Australia, 2015, pp. 19–25.
[12] M.R. Karlsdottir, J. Heinonen, H. Palsson, O.P. Palsson, Life cycle assessment of a geothermal combined heat and power plant based on high temperature utilization, Geothermics 84 (2020), 101727.
[13] C. Liu, S. Wang, J. Ren, Organic Rankine Cycle Driven by Geothermal Heat Source: Life Cycle Techno-Economic–Environmental Analysis, Renewable-Energy-Driven Future, 2021.
[14] D. Scharrer, B. Eppinger, P. Schmitt, J. Zenk, P. Bazan, J. Karl, S. Will, M. Pruckner, R. German, Life cycle assessment of a reversible heat pump–organic Rankine cycle–heat storage system with geothermal heat supply, Energies 13 (12) (2020) 3253.
[15] M. Martín-Gamboa, D. Iribarren, J. Dufour, On the environmental suitability of high-and low-enthalpy geothermal systems, Geothermics 53 (2015) 27–37.
[16] F. Heberle, C. Schifflechner, D. Brüggemann, Life cycle assessment of Organic Rankine Cycles for geothermal power generation considering low-GWP working fluids, Geothermics 64 (2016) 392–400.
[17] L. Gerber, F. Maréchal, Environomic optimal configurations of geothermal energy conversion systems: application to the future construction of Enhanced Geothermal Systems in Switzerland, Energy 45 (1) (2012) 908–923.
[18] A. Stoppato, A. Benato, Life cycle assessment of a commercially available organic rankine cycle unit coupled with a biomass boiler, Energies 13 (7) (2020) 1835.
[19] S. Wang, C. Liu, J. Ren, L. Liu, Q. Li, E. Huo, Carbon footprint analysis of organic rankine cycle system using zeotropic mixtures considering leak of fluid, J. Clean. Prod. 239 (2019), 118095.
[20] S. Gkousis, K. Welkenhuysen, T. Compernolle, Deep geothermal energy extraction, a review on environmental hotspots with focus on geo-technical site conditions, Renew. Sustain. Energy Rev. 162 (2022), 112430.
[21] J.B. Guinée, E. Lindeijer, Handbook on Life Cycle Assessment: Operational Guide to the ISO Standards, Springer Science & Business Media, 2002.
[22] S. Hellweg, L. Milà i Canals, Emerging approaches, challenges and opportunities in life cycle assessment, Science 344 (6188) (2014) 1109–1113.
[23] D. Saner, R. Juraske, M. Kübert, P. Blum, S. Hellweg, P. Bayer, Is it only CO2 that matters? A life cycle perspective on shallow geothermal systems, Renew. Sustain. Energy Rev. 14 (7) (2010) 1798–1813.
[24] A.S. Pratiwi, E. Trutnevyte, Life cycle assessment of shallow to medium-depth geothermal heating and cooling networks in the State of Geneva, Geothermics 90 (2021), 101988.
[25] R. Stemmle, P. Blum, S. Schüppler, P. Fleuchaus, M. Limoges, P. Bayer, K. Menberg, Environmental impacts of aquifer thermal energy storage (ATES), Renew. Sustain. Energy Rev. 151 (2021), 111560.
[26] Z. Günkaya, A. Özdemir, A. Özkan, M. Banar, Environmental performance of electricity generation based on resources: a life cycle assessment case study in Turkey, Sustainability 8 (11) (2016) 1097.
[27] A. Pratiwi, G. Ravier, A. Genter, Life-cycle climate-change impact assessment of enhanced geothermal system plants in the Upper Rhine Valley, Geothermics 75 (2018) 26–39.
[28] C. Tomasini-Montenegro, E. Santoyo-Castelazo, H. Gujba, R. Romero, E. Santoyo, Life cycle assessment of geothermal power generation technologies: an updated review, Appl. Therm. Eng. 114 (2017) 1119–1136.
[29] Y. Wang, Y. Du, J. Wang, J. Zhao, S. Deng, H. Yin, Comparative life cycle assessment of geothermal power generation systems in China, Resour. Conserv. Recycl. 155 (2020), 104670.
[30] E. Buonocore, L. Vanoli, A. Carotenuto, S. Ulgiati, Integrating life cycle assessment and emergy synthesis for the evaluation of a dry steam geothermal power plant in Italy, Energy 86 (2015) 476–487.
[31] E.Y. Gürbüz, O.V. Güler, A. Keçebaş, Environmental impact assessment of a real geothermal driven power plant with two-stage ORC using enhanced exergo-environmental analysis, Renew. Energy 185 (2022) 1110–1123.
[32] A. Paulillo, A. Striolo, P. Lettieri, The environmental impacts and the carbon intensity of geothermal energy: a case study on the Hellisheiði plant, Environ. Int. 133 (2019), 105226.
[33] C. Zuffi, G. Manfrida, F. Asdrubali, L. Talluri, Life cycle assessment of geothermal power plants: a comparison with other energy conversion technologies, Geothermics 104 (2022), 102434.
[34] F. Ruzzenenti, M. Bravi, D. Tempesti, E. Salvatici, G. Manfrida, R. Basosi, Evaluation of the environmental sustainability of a micro CHP system fueled by low-temperature geothermal and solar energy, Energy Convers. Manag. 78 (2014) 611–616.
[35] N. Chaiyat, W. Lerdjaturanon, P. Ondokmai, Life cycle assessment of a combined cooling heating and power generation system, Case Stud. Chem. Environ.Eng. 4 (2021), 100134.
[36] S. Eyerer, C. Schifflechner, S. Hofbauer, W. Bauer, C. Wieland, H. Spliethoff, Combined heat and power from hydrothermal geothermal resources in Germany: an assessment of the potential, Renew. Sustain. Energy Rev. 120 (2020), 109661.
[37] K. Menberg, F. Heberle, C. Bott, D. Brüggemann, P. Bayer, Environmental performance of a geothermal power plant using a hydrothermal resource in the Southern German Molasse Basin, Renew. Energy 167 (2021) 20–31.
[38] M. Irl, C. Wieland, H. Spliethoff, Auswertung von Langzeitbetriebsdaten verschiedener Tauchkreiselpumpen und Auswirkungen von Säuerungen, Der digitale Geothermiekongress, Online, 2020 (in German).
[39] J. Bonafin, A. Duvia, C. Zulfikar, Operations Update of European Geothermal Binary Units Delivered by Turboden, European Geothermal Congress 2019, Den Haag, The Netherlands, 2019.
[40] A. McCulloch, Life cycle inventory analysis of the production of a high-performance foam blowing agent HFC-245fa (1, 1, 1, 3, 3-Pentafluoropropane), J. Cell. Plast. 46 (1) (2010) 57–72.
[41] A. Baral, R. Minjares, R. Urban, Upstream Climate Impacts from Production of R-134a and R-1234yf Refrigerants Used in Mobile Air Conditioning Systems, International Council on Clean Transportation, 2013.
[42] T. Eller, F. Heberle, D. Brüggemann, Transient simulation of geothermal combined heat and power generation for a resilient energetic and economic evaluation, Energies 12 (5) (2019) 894.
[43] T. Eller, F. Heberle, D. Brüggemann, Evaluation of different power plant concepts for geothermal heat and power production, Proceed.Eur. Geothermal Congr. (2019).
[44] M.L. Parisi, M. Douziech, L. Tosti, P. Pérez-López, B. Mendecka, S. Ulgiati, D. Fiaschi, G. Manfrida, I. Blanc, Definition of LCA guidelines in the geothermal sector to enhance result comparability, Energies 13 (14) (2020) 3534.
[45] F. Heberle, D. Brüggemann, Exergy based fluid selection for a geothermal Organic Rankine Cycle for combined heat and power generation, Appl. Therm. Eng. 30 (11–12) (2010) 1326–1332.
[46] D. Fiaschi, A. Lifshitz, G. Manfrida, D. Tempesti, An innovative ORC power plant layout for heat and power generation from medium- to low-temperature geothermal resources, Energy Convers. Manag. 88 (2014) 883–893.
[47] S. Van Erdeweghe, J. Van Bael, B. Laenen, W. D'Haeseleer, Optimal configuration for a low-temperature geothermal CHP plant based on thermoeconomic optimization, Energy 179 (2019) 323–335.
[48] S. Eyerer, F. Dawo, C. Wieland, H. Spliethoff, Advanced ORC architecture for geothermal combined heat and power generation, Energy 205 (2020), 117967.
[49] Geothermie Unterhaching. https://www.geothermie-unterhaching.de/cms/geothermie/web.nsf/gfx/0189A5952BAEB5E8C1258183003FA71A/$file/Datenblatt%20Geothermie%20Unterhaching%202017.pdf. (Accessed 2 March 2022).
[50] Bayernwerk. https://www.poing.de/fileadmin/eigene_dateien/05_Bauen_Umwelt/Energie_Klima/Energie/Geothermie/210922_Waermenetz_der_Bayernwerk_Natur_GmbH_in_Poing_Statusbericht.pdf. (Accessed 2 March 2022).
[51] VDI 4655, Referenzlastprofile von Wohngebäuden für Strom, Heizung und Trinkwarmwasser sowie Referenzerzeugungsprofile für Fotovoltaikanlagen, Verein Deutscher Ingenieure e.V., 2021.
[52] VDI 3807, Verbrauchskennwerte für Gebäude, Verein Deutscher Ingenieure e.V., 2014.
[53] https://www.dwd.de/DE/klimaumwelt/cdc/cdc_node.html. (Accessed 10 January 2022).
[54] ISO 14040: Environmental Management – Life Cycle Assessment – Principles and Framework, International Organization for Standardization (ISO), 2006.
[55] ISO 14044: Environmental Management – Life Cycle Assessment – Requirements and Guidelines, International Organization for Standardization (ISO), 2018.
[56] O. Jolliet, M. Margni, R. Charles, S. Humbert, J. Payet, G. Rebitzer, R. Rosenbaum, Impact 2002+: a new life cycle impact assessment methodology, Int. J. Life Cycle Assess. 8 (6) (2003) 324–330.
[57] Swiss centre for life cycle inventories, Ecoinvent Database v3.5 (2018).
[58] M.R. Karlsdottir, J. Heinonen, H. Palsson, O.P. Palsson, High-temperature geothermal utilization in the context of European energy policy—implications and limitations, Energies 13 (12) (2020) 3187.
[59] K. Bettgenhaeuser, T. Boermans, Environmental Impacts of Heating Systems in Germany, Umweltwirkung von Heizungssystemen in Deutschland, 2011.

[60] A. Aquino, F. Scrucca, E. Bonamente, Sustainability of shallow geothermal energy for building air-conditioning, Energies 14 (21) (2021) 7058.
[61] A.C. Violante, F. Donato, G. Guidi, M. Proposito, Comparative life cycle assessment of the ground source heat pump vs air source heat pump, Renew. Energy 188 (2022) 1029–1037.
[62] C. Tomasetta, Life Cycle Assessment of Underground Thermal Energy Storage Systems: Aquifer Thermal Energy Storage Verus Borehole Thermal Energy Storage, Università Ca'Foscari Venezia, 2013.
[63] P. Bayer, D. Saner, S. Bolay, L. Rybach, P. Blum, Greenhouse gas emission savings of ground source heat pump systems in Europe: a review, Renew. Sustain. Energy Rev. 16 (2) (2012) 1256–1267.
[64] D. Fiaschi, G. Manfrida, B. Mendecka, L. Tosti, M.L. Parisi, A comparison of different approaches for assessing energy outputs of combined heat and power geothermal plants, Sustainability 13 (8) (2021) 4527.
[65] P. Icha, T. Lauf, G. Kuhs, Entwicklung der spezifischen Kohlendioxid-Emissionen des deutschen Strommix in den Jahren 1990 - 2020, 2021.
[66] Swiss centre for life cycle inventories, Ecoinvent Database v2.2 (2010).